

University of Groningen

## Photoactivation provides a mechanistic explanation for pan-assay interference behaviour of 2-aminopyrroles in lipoxygenase inhibition

Guo, Hao; Eleftheriadis, Nikolaos; Rohr-Udilova, Nataliya; Dömling, Alexander; Dekker, Frank J

*Published in:*  
European Journal of Medicinal Chemistry

*DOI:*  
[10.1016/j.ejmech.2017.07.047](https://doi.org/10.1016/j.ejmech.2017.07.047)

**IMPORTANT NOTE: You are advised to consult the publisher's version (publisher's PDF) if you wish to cite from it. Please check the document version below.**

*Document Version*  
Publisher's PDF, also known as Version of record

*Publication date:*  
2017

[Link to publication in University of Groningen/UMCG research database](#)

*Citation for published version (APA):*

Guo, H., Eleftheriadis, N., Rohr-Udilova, N., Dömling, A., & Dekker, F. J. (2017). Photoactivation provides a mechanistic explanation for pan-assay interference behaviour of 2-aminopyrroles in lipoxygenase inhibition. *European Journal of Medicinal Chemistry*, 139(20), 633-643. <https://doi.org/10.1016/j.ejmech.2017.07.047>

### Copyright

Other than for strictly personal use, it is not permitted to download or to forward/distribute the text or part of it without the consent of the author(s) and/or copyright holder(s), unless the work is under an open content license (like Creative Commons).

The publication may also be distributed here under the terms of Article 25fa of the Dutch Copyright Act, indicated by the "Taverne" license. More information can be found on the University of Groningen website: <https://www.rug.nl/library/open-access/self-archiving-pure/taverne-amendment>.

### Take-down policy

If you believe that this document breaches copyright please contact us providing details, and we will remove access to the work immediately and investigate your claim.

Downloaded from the University of Groningen/UMCG research database (Pure): <http://www.rug.nl/research/portal>. For technical reasons the number of authors shown on this cover page is limited to 10 maximum.



## Research paper

## Photoactivation provides a mechanistic explanation for pan-assay interference behaviour of 2-aminopyrroles in lipoxygenase inhibition

Hao Guo<sup>a</sup>, Nikolaos Eleftheriadis<sup>a</sup>, Nataliya Rohr-Udilova<sup>b</sup>, Alexander Dömling<sup>c</sup>, Frank J. Dekker<sup>a,\*</sup><sup>a</sup> Chemical and Pharmaceutical Biology, Groningen Research Institute of Pharmacy (GRIP), University of Groningen, Groningen, The Netherlands<sup>b</sup> Division of Gastroenterology and Hepatology, Department of Internal Medicine III, Medical University of Vienna, Austria<sup>c</sup> Drug Design, Groningen Research Institute of Pharmacy, University of Groningen, Groningen, The Netherlands

## ARTICLE INFO

## Article history:

Received 23 May 2017

Received in revised form

13 July 2017

Accepted 22 July 2017

Available online 24 July 2017

## Keywords:

15-Lipoxygenase-1

2-Aminopyrrole

Photoactivation

Pan assay interference compounds (PAINS)

## ABSTRACT

Human 15-lipoxygenase-1 (h-15-LOX-1) is a promising drug target in inflammation and cancer. In this study substitution-oriented screening (SOS) has been used to identify compounds with a 2-aminopyrrole scaffold as inhibitors for h-15-LOX-1. The observed structure activity relationships (SAR) proved to be relatively flat. IC<sub>50</sub>'s for the most potent inhibitor of the series did not surpass 6.3 μM and the enzyme kinetics demonstrated uncompetitive inhibition. Based on this, we hypothesized that the investigated 2-aminopyrroles are pan assay interference compounds (PAINS) with photoactivation via a radical mechanism. Our results demonstrated clear photoactivation of h-15-LOX-1 inhibition under UV and visible light. In addition, the investigated 2-aminopyrroles decreased viability of cultured human hepatocarcinoma cells HCC-1.2 in a dose-dependent manner with LD<sub>50</sub> ranging from 0.55 ± 0.15 μM (**21B10**) to 2.75 ± 0.91 μM (**22**). Taken together, this indicates that photoactivation can play an important role in the biological activity of compounds with a 2-amino-pyrrole scaffold as investigated here.

© 2017 Elsevier Masson SAS. All rights reserved.

## 1. Introduction

Many diseases that are predominant in the aging western population have an immunological component. For example, immunological responses play a key role in cancer, which is the second-leading cause of death, resulting in about 8.2 million (14.6%) of human deaths in total [1–3]. Therefore, it is important to investigate the molecular mechanisms driving the immune system in aging-related diseases with an immunological component.

Enzymes that produce signaling molecules are key regulators of molecular mechanisms involved in immune responses and cell proliferation. Therefore, the development of novel selective molecules to inhibit enzyme activity in model systems for these diseases is urgently needed.

One enzyme that has been increasingly associated with regulation of the immune system in various conditions is human 15-lipoxygenase-1 (h-15-LOX-1) [4–7]. h-15-LOX-1 belongs to the heterogeneous family of Lipoxygenases (LOXs), which are non-heme

iron-containing enzymes that regio- and stereospecifically introduce oxygen into 1,4 polyunsaturated fatty acids to produce the corresponding hydroperoxy derivatives. The primary lipid peroxidation products from arachidonic acid (AA) and linoleic acid (LA) are hydroperoxyeicosatetraenoic acid (HpETE) and hydroperoxyoctadecadienoic acid (HpODE), respectively. These peroxides can be reduced to the respective hydroxy fatty acids, such as hydroxyeicosatetraenoic acid (HETE), hydroxyoctadecadienoic acid (HODE), lipoxins, eoxins, and leukotrienes [6,8]. In mammals, LOXs are classified according to their positional specificity of arachidonic acid oxygenation at carbons 5, 8, 9, 11, 12 or 15. Meanwhile, the basic catalytic mechanism of h-15-LOX-1 is generally accepted to be as follows. The iron (III) containing active site of activated 15-LOX causes single electron oxidation of arachidonic or linoleic acid that is bound to the active site, resulting in a carbon centered radical that reacts with O<sub>2</sub>, and generates a new radical. Then, the radical endoperoxide oxidizes the iron(II) to iron(III) for the next catalytic cycle [5,9].

The enzyme, h-15-LOX-1 and its metabolites have been implicated in numerous diseases with an immunological component such as asthma [10], atherogenesis [11], diabetes [12,13], stroke [14], Alzheimer's disease [15], Parkinson's disease [16], and cancer

\* Corresponding author.

E-mail address: [f.j.dekker@rug.nl](mailto:f.j.dekker@rug.nl) (F.J. Dekker).

[17–19]. In cancer, many studies have shown that h-15-LOX-1 and its metabolites have a versatile role in cancer incidence, progression, and invasion [20,21]. In this study, human hepatocarcinoma cell line HCC-1.2 was used as an *in vitro* model to verify the role of h-15-LOX inhibition in cancer [22].

The tremendously increasing interest in the functional behavior of h-15-LOX-1 has triggered experimental efforts in the development of potent and selective h-15-LOX-1 inhibitors [11,23]. Despite significant investments, none of the known 15-LOX inhibitors has reached clinical trials. Frequently, the h-15-LOX-1 inhibitors have limited potency and/or unfavorable physical chemical properties such as high logP values. Purine-based compound (**6b**) was the first class of 15-LOX inhibitors discovered ( $IC_{50} = 96 \mu\text{M}$ ) in 2002 (Fig. 1) [24]. Compound **6640337** has been identified by structure-based virtual screening, however, its selectivity among lipoxygenase isoenzymes remains limited [25]. Other inhibitors were identified that include indole or oxazole moieties. Researchers from Bristol-Myers Squibb (BMS) identified another potent indole-based inhibitor **371** ( $IC_{50} = 0.006 \mu\text{M}$ ) [26]. Recently, compound **ML351** with an oxazole scaffold was identified and demonstrated nanomolar potency ( $IC_{50} = 0.2 \mu\text{M}$ ) against human 12/15-LOX [14]. Furthermore, our group recently reported the discovery of inhibitors **N247** and **ThioLox** adding to the success of indole- and thiophene-based inhibitors for h-15-LOX-1 ( $IC_{50} = 0.09$  and  $12.4 \mu\text{M}$ ) [27,28]. However, to explore the utility of this enzyme, further inhibitors with new chemotypes and improved physical-chemical properties are needed [29].

In this study, the 2-aminopyrrole scaffold was selected as a starting point for identification of novel h-15-LOX-1 inhibitors because of its similarity with the indole inhibitor **N247**. A substitution-oriented screening (SOS) of about 200 2-aminopyrrole inhibitors has been done (Fig. 2) in order to optimize binding to h-15-LOX-1 [27,28]. Structure-activity relationships (SAR) and enzyme kinetics were evaluated. The compound class investigated here proved to be photoactivatable inhibitors of both, lipoxygenase activity and viability of HCC-1.2 hepatocarcinoma cell. Presumably, this photoactivation represents a non-specific inhibitory mechanism suggesting that these compounds are pan assay interfering compounds (PAINS) [30,31].

## 2. Results and discussion

### 2.1. Fragment screening and hit identification

The substitution-oriented screening (SOS) for 15-LOX-1

inhibitors was done by using a library of 200 fragments containing 192 2-aminopyrroles and 8 2-aminoindoles with diverse substitution patterns (Fig. S1).

The screening for h-15-LOX-1 inhibition was done by using a UV absorption assay for the h-15-LOX-1 product, 13(S)-HODE ( $\lambda_{\text{max}} 234 \text{ nm}$ ) formed by enzymatic conversion from linoleic acid [27,32]. This assay was performed in a 96-well format, which is well suited for medium-throughput screening,  $IC_{50}$  measurements and enzyme kinetics studies. Using this assay, the SOS library was screened, and three compounds that provided more than 80% inhibition of the enzyme's activity at  $50 \mu\text{M}$  were identified. Compounds with three distant structural scaffolds were identified (Fig. 2). Comparison of the scaffolds showed that scaffold **II** and **III** exhibit the best potency against h-15-LOX-1 of with  $22.3 \pm 4.6 \mu\text{M}$  and  $32.8 \pm 5.1 \mu\text{M}$ , respectively. We decided to move on with scaffold **III** due to better properties and the lack of the indole moiety as present in the previously identified inhibitor **N247** (Fig. 1) [27]. The relative potency of compound **1** (**21B10**) with scaffold **III** was determined and provided an  $IC_{50}$  value of  $12.8 \pm 4.0 \mu\text{M}$ .

Diversely substituted pyrroles with various  $R^1$ ,  $R^2$  and  $R^3$  groups were present in the SOS screening. To begin with, comparison of 45 compounds in the library (Fig. S2) indicated that the 4-substitution on region  $R^3$  did not greatly change the inhibitory potency, and even led to potency loss in some compounds (Fig. S2. **C15**, **B19**, **C25**, **B31**). Diverse halogenic and methoxyl substitution patterns showed that this kind of substituent groups were less potent relative to the inhibitory potency against h-15-LOX-1. This indicated that an unsubstituted benzene ring is the most optimal functionality identified in the  $R^3$  region. For  $R^2$ , 2,4-dichlorophenyl moiety provided the most potent inhibitors. For  $R^1$ , the library consisted of little variation that more information will be got from further synthesis.

### 2.2. Structure-based design

To investigate the structure-activity relationship (SAR), we synthesized a number of h-15-LOX-1 inhibitors as variants of inhibitor **1** (**21B10**), as shown in Tables 1 and 2 and Fig. 3 (1–30). The synthesis of 2-aminopyrrole analogues proceeded by application of a multicomponent reaction resulting 2-aminopyrroles (Scheme 1) with various  $R^1$ ,  $R^2$  and  $R^3$  substituents. The crude product was purified by column chromatography eluting with 20% ethyl acetate in  $\text{CH}_2\text{Cl}_2$  to reach a general yield from 22% to 40%.

Initially, region  $R^2$  and  $R^3$  were held constant while region  $R^1$  was explored for modification (Table 1). Replacement of the 3,4-

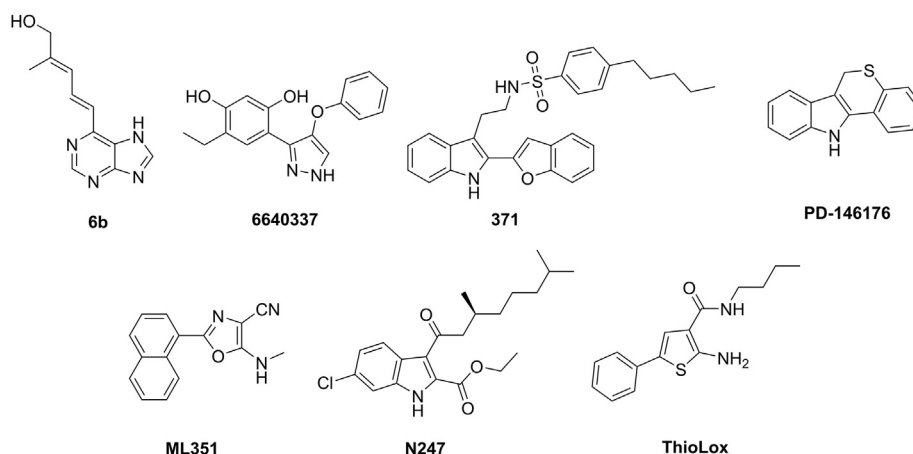
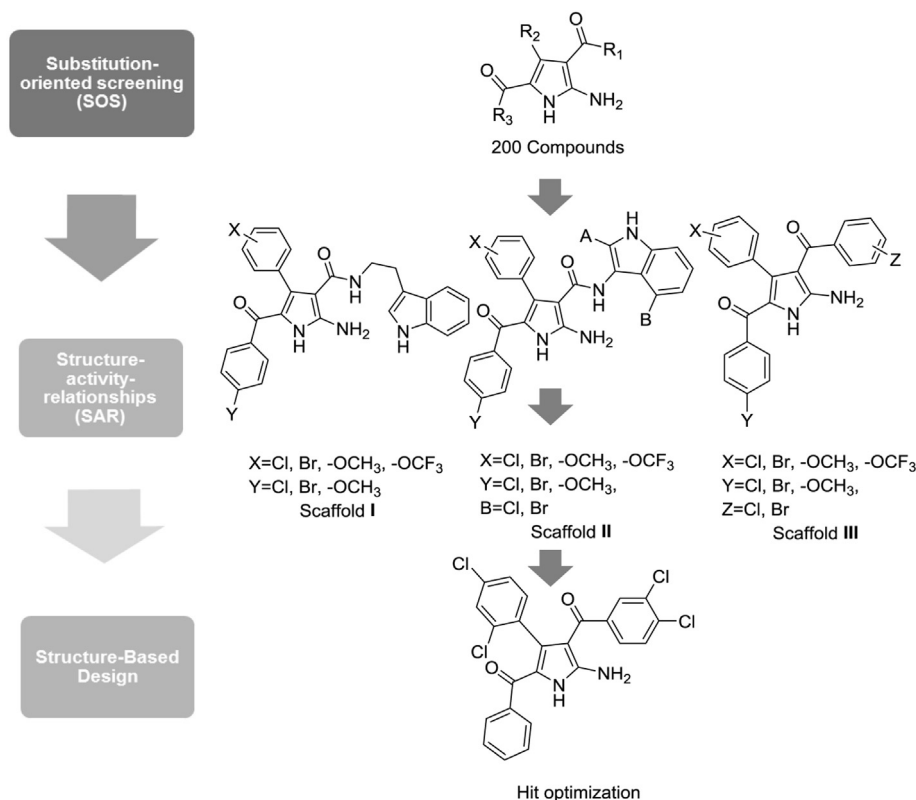


Fig. 1. Examples of previously reported 15-LOX inhibitors.



**Fig. 2.** Workflow as applied in this study starting with a Substitution-oriented screening (SOS) of a 2-aminopyrrole library for 15-LOX-1 inhibitory potency to identify hit compounds. Subsequent hit optimization by identification of structure-activity-relationships (SAR) and structure-based design.

**Table 1**

IC<sub>50</sub> values against h-15-LOX-1 with different variations in R<sup>1</sup> and R<sup>2</sup> position based on compound **21B10** (Analogues **1–13**).

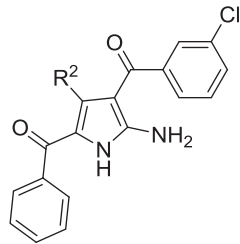
Compound	R <sup>1</sup>	IC <sub>50</sub> (μM)	Compound	R <sup>2</sup>	IC <sub>50</sub> (μM)
<b>1(21B10)</b>	3,4-dichlorophenyl	12.8 ± 3.3	<b>10</b>	naphthalen-1-yl	36.1 ± 2.3
<b>2</b>	4-chlorophenyl	>100	<b>11</b>	naphthalen-2-yl	>100
<b>3</b>	3-chlorophenyl	6.9 ± 1.7	<b>12</b>	hydrogen	11.8 ± 2.3
<b>4</b>	3-bromophenyl	6.3 ± 1.1	<b>13</b>	2,6-difluorophenyl	>100
<b>5</b>	3-fluorophenyl	>100			
<b>6</b>	<i>m</i> -tolyl	>100			
<b>7</b>	phenyl	>100			
<b>8</b>	thiophen-2-yl	>100			
<b>9</b>	amine	>100			

dichlorophenyl (**1**) with a 4-chlorophenyl (**2**) functionality provided an inactive compound, whereas replacement by 3-chlorophenyl (**3**) or 3-bromophenyl (**4**) provided nearly twofold improved potency for inhibition of h-15-LOX-1. Remarkably, the 3-fluorophenyl (**5**) and 3-methylphenyl (**6**) derivatives lost their potency against h-15-LOX-1, which suggest involvement in halogen bonding. Several other modifications at this R<sup>1</sup> region including unsubstituted or other heterocyclic rings (**7–9**) resulted in a complete loss of activity against h-15-LOX-1. Taken together these

results suggest that halogen- and hydrogen-bonding is important for inhibition of h-15-LOX-1 by this type of compounds.

Having explored modifications to the 3-chlorobenzoyl moiety on region R<sup>1</sup>, further structure-activity relationships around region R<sup>2</sup> were studied (Table 2, Fig. 3). In the pyrrole 4-position, the 2,4-dichlorophenyl was replaced to 2-naphthyl (**12**) or 2,4-dihydroxyphenyl (**22**) groups, which resulted in molecules with comparable, albeit slightly higher, potencies than **1** (IC<sub>50</sub> = 11.8 ± 2.3 and 8.3 ± 1.1 μM, respectively). Replacements by

**Table 2**  
IC<sub>50</sub> values against h-15-LOX-1 with different variations in R<sub>2</sub> position based on compound **21B10** (Analogues **14–27**, **28**, **29**, **30**).



Compound	R <sup>2</sup>	IC <sub>50</sub> (μM)	Compound	R <sup>2</sup>	IC <sub>50</sub> (μM)
<b>14</b>	hydrogen	41.8 ± 8.5	<b>21</b>	2,4-difluorophenyl	44.1 ± 4.7
<b>15</b>	1,1'-biphenyl	>100	<b>22</b>	2,4-dihydroxyphenyl	8.3 ± 1.1
<b>16</b>	phenyl	67.9 ± 5.9	<b>23</b>	2,4-dimethylphenyl	39.0 ± 8.3
<b>17</b>	3,4-dichlorophenyl	35.7 ± 7.0	<b>24</b>	benzo[d][1,3]dioxol-5-yl	>100
<b>18</b>	4-chlorophenyl	>100	<b>25</b>	pyridin-4-yl	>100
<b>19</b>	2-chlorophenyl	>100	<b>26</b>	pyridin-3-yl	>100
<b>20</b>	3-chlorophenyl	>100	<b>27</b>	2,4-dimethoxyphenyl	58.2 ± 6.8

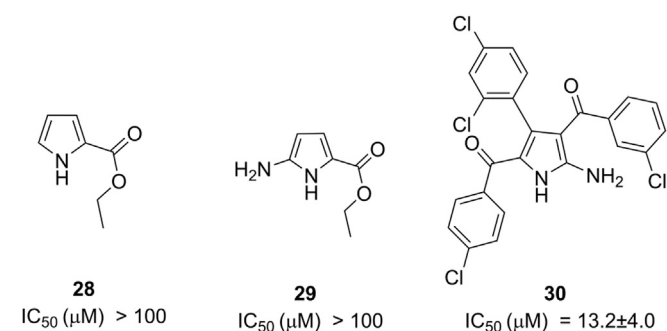
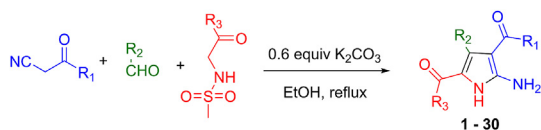


**Fig. 3.** IC<sub>50</sub> values against h-15-LOX-1 with smaller variations (**28**, **29**) and variation in R<sub>3</sub> position (**30**) based on compound **21B10**.



**Scheme 1.** Synthetic Route to Compounds **1–30**. Reagents and conditions: aldehydes, cyanoacetic acid derivatives, methylsulfonylamidoacetophenone, K<sub>2</sub>CO<sub>3</sub>, EtOH, reflux, 12 h.

hydrogen (**10**, **14**) resulted in reduced inhibitory potency against h-15-LOX-1. Further chain-length extension, such as biphenyl group (**15**) led to inactivity against h-15-LOX-1. Also, changing the numbers and positions of substituent groups on the phenyl group decreased the inhibitory potency (**13**, **16–21**, **23**, **27**). Another heterocyclic handle such as 3-pyridine (**26**) and 4-pyridine (**25**) replacements for modulating their physical property showed a complete loss of inhibitory potency against h-15-LOX-1.

Taken together, it can be concluded that 2,4-dichlorophenyl (**3**) and 2,4-dihydroxyphenyl (**22**) groups in the R<sup>2</sup> position appeared to be optimal for h-15-LOX-1 inhibition by this type of compounds. Other variations in size and electrostatics of the substituents in this position decreased the inhibitory potency. Compound **28**, **29** minimally substituted pyrrole core were inactive against h-15-LOX-1 activity.

### 2.3. Cytotoxicity study on human hepatocarcinoma HCC-1.2 cell line

After establishing the SAR profile against h-15-LOX-1, we turned our attention to the cellular level and selected eight 2-aminopyrroles for evaluation of cytotoxicity (Fig. S5). All selected compounds exhibited similar LD<sub>50</sub>'s indicating that the cytotoxic potency is not directly linked to h-15-LOX-1 inhibition as shown in Table 3.

### 2.4. Photoactivation study of selected compounds against h-15-LOX-1 and HCC-1.2 cell line

Our findings on flat SAR for this compound class together with observed cytotoxicity triggered our attention. The 2-aminopyrroles applied here contain two ketone functionalities flanked by aromatic groups. This is similar to benzophenone that consists of a ketone flanked by two aromatic groups. For benzophenones, it has been described that photoactivation generates bi-radicals that are highly reactive towards proteins and other biomolecules [33,34]. In the compound class under investigation, there are two ketones between aromatic functionalities that could potentially undergo photoactivation according to a mechanism similar to benzophenone.

We aimed to experimentally verify the hypothesis that the 2-aminopyrroles under investigation are prone to photoactivation in their effects on h-15-LOX-1 activity and HCC-1.2 cell viability. The light- and time-dependence were investigated for selected 2-

**Table 3**

Cytotoxicity study on selected compounds against hepatocarcinoma HCC-1.2 cells: all compounds were equal in their cytotoxicity for this particular type of cancer cells despite their differences in potency for h-15-LOX-1.

Compound	LD <sub>50</sub> (μM)
<b>21B10</b>	0.55 ± 0.15
<b>2</b>	1.05 ± 0.31
<b>3</b>	0.69 ± 0.14
<b>4</b>	1.64 ± 0.72
<b>6</b>	1.04 ± 0.32
<b>12</b>	2.64 ± 0.12
<b>21</b>	0.99 ± 0.60
<b>22</b>	2.75 ± 0.91

aminopyrroles. Spectral analysis revealed that this type of 2-aminopyrroles have a broad UV absorption band with a maximum at 390 nm (Fig. S6). Since this molecule still considerably absorbs at 365 nm, this wavelength was chosen for UV irradiation. Because of the broad UV absorption band, we chose day light as another condition. As a control we also included irradiation with 254 nm in our study.

The inhibition of h-15-LOX-1 by 2-aminopyrrole **1** and **3** proved to be both light- and time-dependent (Fig. 4). Upon exposure to 365 nm UV light, the inhibition rate increased clearly over the time. Ten-minute irradiation provided inhibition values clearly higher as compared to pre-incubation in the darkness. Exposure of the sample to day-light in the pre-incubation phase provides higher inhibition values already at much shorter times (2 min). Furthermore, activity of h-15-LOX-1 after 2-min irradiation at 365 nm was much higher as compared to day light irradiation of the same duration. This means that UV irradiation at 365 nm was less efficient as compared to day light. However, the difference between UV and day light almost disappeared after 10-min irradiation. The potential explanation for the observed results was the broad UV absorption band of 2-aminopyrroles and that 365 nm was not the maximum absorbance of this molecule. Whereas the change of enzyme activity in the dark showed little change, that was nearly 80% after 10-min incubation in the end. As a control we also included irradiation with 254 nm UV light. Under these conditions no photoactivation of inhibition was observed. This indicates that the h-15-LOX-1 assay as applied here employing UV absorbance detection at 254 nm does not interfere with photoactivation. Thus, our findings showed that the inhibitory potency of compounds **1** and **3** against h-15-LOX-1 is time-dependent upon pre-incubation under 365 nm UV light. Both UV-light and day-light exposure

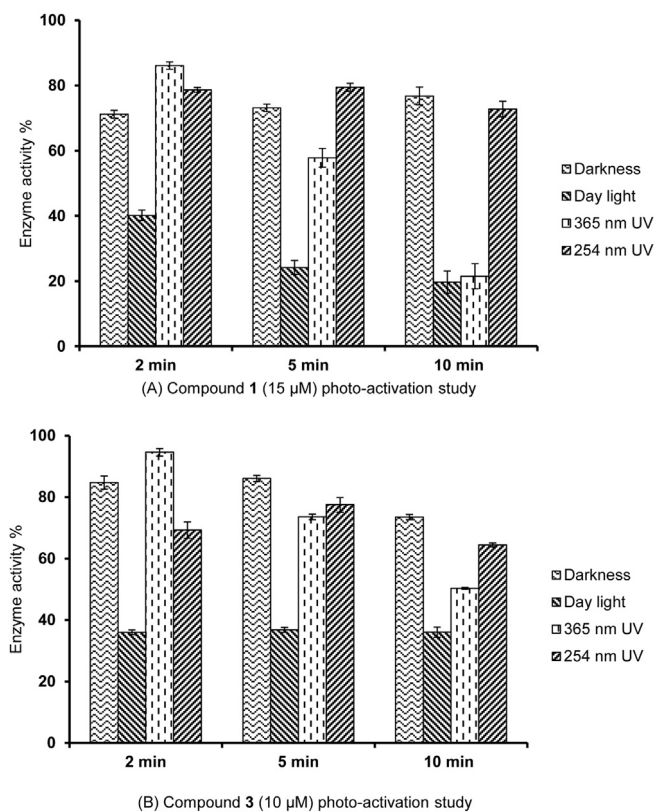


**Fig. 4.** Enzyme photoactivation study on compound **1** and **3** with different incubation time and environment. Data are presented as mean values  $\pm$  SD of 3 independent experiments.

during pre-incubation improves inhibition of h-15-LOX-1. These findings are in line with a photoactivation mechanism for enzyme inhibition of h-15-LOX-1 by this type of 2-aminopyrroles. Presumably, the photoactivation via the proposed mechanism for the formation of bi-radicals is highly dependent on the electronic properties of the substitution pattern of the respective inhibitor. This could explain a major component of the observed structure activity relationships in Tables 1 and 2. Nevertheless, the shape and electronic properties of the inhibitors also play an important role in binding to enzyme active site, which is an important contributor to enzyme inhibition.

Further experiments were performed on cytotoxicity by selected compounds, **3**, **6** and **21**, which were either potent, moderate or non-active against h-15-LOX-1, respectively (Fig. 5). Light has no impact on the activity of compound **21**. In contrast, compound **6** showed significant differences between incubation in the dark and daylight between 0.4 and 10 µM. For compound **3** the differences are less clear but they are significant between 1 and 10 µM. These findings confirmed photoactivation of this type of compounds is also possible in cell-based studies.

### 2.5. Enzyme kinetics h-15-LOX-1 inhibition

Inhibitor **1** was subjected to enzyme kinetic analysis in order to explore the inhibitory mechanism of h-15-LOX-1 inhibition. The Michaelis-Menten and Lineweaver-Burk plot are shown in Fig. 6A and B and the enzyme kinetic parameters derived from Fig. 6A are shown in Table 4. Compound **1** causes a decrease both in  $K_m$  value and  $V_{max}$ , which means that 2-aminopyrroles demonstrate

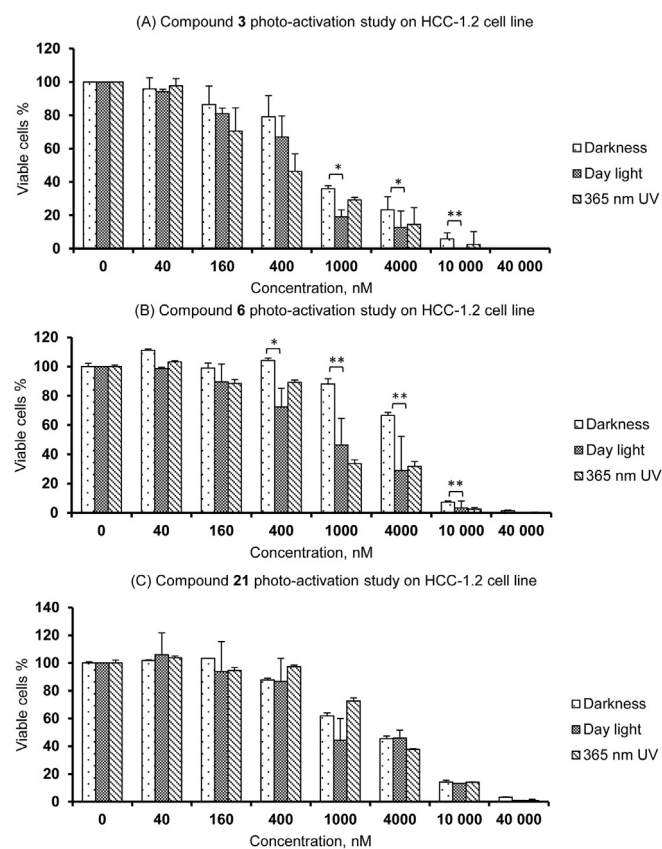


**Fig. 5.** Cytotoxicity photoactivation study on selected compounds (**3**, **6**, **21**) against hepatocarcinoma HCC-1.2 cells with different irradiation conditions and inhibitor concentrations. Data are presented as mean values  $\pm$  SD of 3 independent experiments. \* $p < 0.01$ ; \*\* $p < 0.005$ .

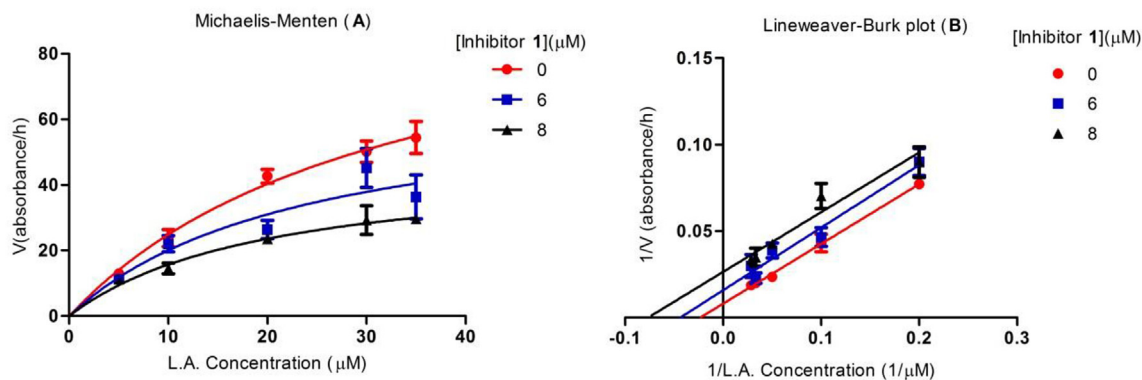


**Fig. 6.** Steady-State kinetic characterization of human 15-lipoxygenase-1 (15-LOX-1) in the presence of different concentrations of compound **1**: A) Michaelis-Menten representation and B) Lineweaver-Burk representation ( $n = 3$ ).

**Table 4**

Enzyme kinetic parameters for inhibition of h-15-LOX-1 by inhibitor **1**.

Compound <b>1</b> ( $\mu\text{M}$ )	$K_m^{app}$ ( $\mu\text{M}$ )	$V_{max}^{app}$ (absorbance/h)
0	$32.67 \pm 12.23$	$106.10 \pm 40.95$
6	$23.98 \pm 11.57$	$68.18 \pm 23.05$
8	$20.04 \pm 8.98$	$47.21 \pm 12.62$

All the  $p$ -values were calculated in GraphPad Prism 5.0 after linear regression fit. The  $p$ -values show that the slopes are significantly non-zero ( $p$ -value < 0.05).

uncompetitive inhibition of h-15-LOX-1. Uncompetitive inhibition indicates that this inhibitor binds to the enzyme-substrate complex (ES) and not to the free enzyme (E). This observation together with the observation that inhibitor **1** is prone to photoactivation presumably via the formation of bi-radicals (Fig. 7A) raises the hypothesis that these bi-radicals interfere with the catalytic cycle of linoleic acid conversion by h-15-LOX-1 (Fig. 7B). This type of uncompetitive inhibition has been observed previously for redox

active h-15-LOX-1 inhibitors. Possibly, the allyl-peroxide intermediate could react with inhibitor **1** in a photoactivation dependent manner resulting in inhibition of the enzyme activity. Taken together, this observed uncompetitive enzyme inhibition mechanism does not contradict the idea of a photoactivation mechanism in which formation of bi-radicals plays a role.

Actually, we noted that, 2-aminopyrroles become increasingly prevalent in recent studies as a promising start for many known targets and bioactivities [35–40]. This is particularly relevant because 2-aminopyrrole inhibitors have been identified as hits for a number of targets. Taken together, our observations in this study demonstrate that careful analysis of the mechanism of inhibition of this type of compounds is needed. Anticipation on a potential PAINS character would be needed for this type of compounds.

In conclusion, the 2-aminopyrroles investigated here proved to exhibit photoactivatable characteristics presumably originating from the formation of bi-radicals as described for benzophenone. Such a mechanism would imply non-selective binding of this

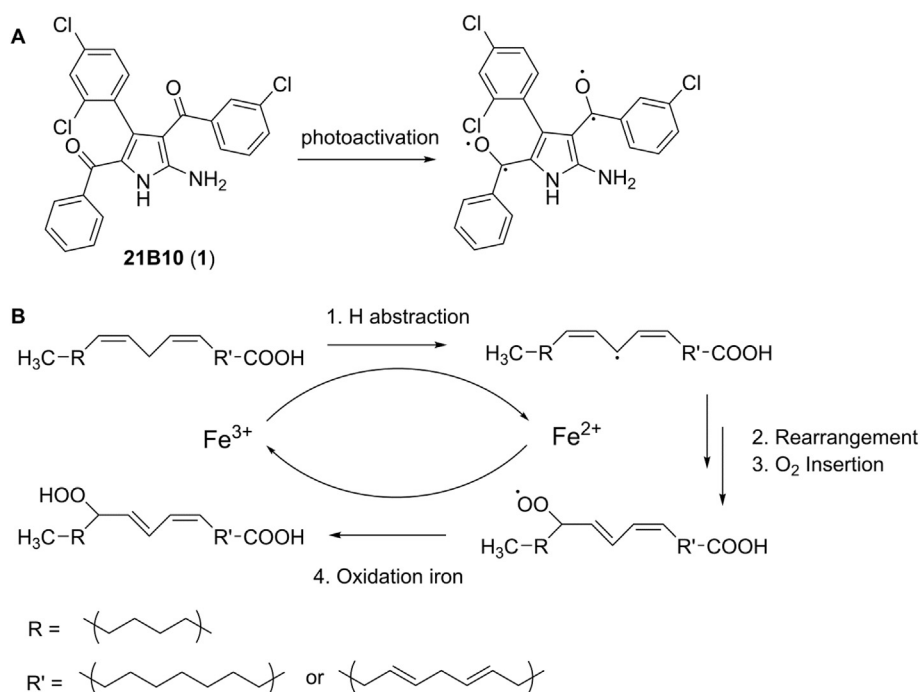


**Fig. 7.** A) Proposed formation of bi-radicals in the ketone functionalities of inhibitor **1** upon photoactivation. B) catalytic cycle for the conversion of arachidonic acid or linoleic acid by LOX activity. Iron(III) causes single electron oxidation of arachidonic acid or linoleic acid and converts into iron(II). This results in a carbon centered radical that combines with  $\text{O}_2$ , which generates a new radical. The radical allyloperoxide oxidizes the iron(II) to iron(III) for the next catalytic cycle.

compound class in biological systems, which is in line with the findings in this study. Recently, many compounds have been described as having a PAINS character without a clear description of the underlying mechanisms [30]. In this study we provide evidence that photoactivation can play a role in the biological activity of small molecules. This could potentially be a mechanism for PAINS behavior and could also cause irreproducible results if the light exposure is not taken into account. However, photoactivation of compounds can be also potentially useful as in case of photodynamic therapy [41]. Therefore, we argue for more attention to this issue in enzyme inhibition studies and in other biological investigations.

### 3. Conclusions

In this study, our initial effort was to discover a novel potent and selective h-15-LOX-1 inhibitor by screening a library of 2-aminopyrroles. Despite optimization, the potency of this type of inhibitors remains limited to the micromolar range. Additionally, we found that viability of HCC-1.2 cells was inhibited by this type of compounds. Afterwards, the similarity to benzophenone triggered us to investigate the photoactivation. Indeed, we found photoactivation at the enzymatic and cellular level after the exposure to UV-irradiation (365 nm) and visible light. This suggested that the 2-aminopyrroles might act as pan assay interfering substances, presumably acting via a radical mechanism.

In view of our findings, we argue for more vigilance with respect to potential photoactivation of small molecule inhibitors, in particular if compounds contain a ketone group in between of two aromatic functionalities. All in all, these photoactivation properties should carefully be considered in the application of this type of 2-aminopyrroles in medicinal chemistry projects.

### 4. Experimental section

#### 4.1. Chemistry

##### 4.1.1. General

All reagents, solvents and catalysts were purchased from commercial sources (Acros Organics, Sigma-Aldrich and abcr GmbH, Netherlands) and used without purification. All reactions were performed in oven dried flasks open to the atmosphere, or under nitrogen, and monitored by thin layer chromatography on TLC precoated (250  $\mu\text{m}$ ) silica gel 60 F254 glassbacked plates (EMD Chemicals Inc.). Visualization was achieved using UV light. Alternatively, non UV-active compounds were detected after staining with potassium permanganate. Flash column chromatography was performed on silica gel (32–63  $\mu\text{m}$ , 60  $\text{\AA}$  pore size).  $^1\text{H}$  NMR (500 MHz) and  $^{13}\text{C}$  NMR (126 MHz) spectra were recorded with a Bruker Avance 4-channel NMR Spectrometer with TXI probe. Chemical shifts ( $\delta$ ) are reported in ppm relative to the Tetramethylsilane (TMS) internal standard. Abbreviations are as follows: s (singlet), d (doublet), t (triplet), q (quartet), m (multiplet). Fourier Transform Mass Spectrometry (FTMS) and electrospray ionization (ESI) were done on an Applied Biosystems/SCIEX API3000-triple quadrupole mass spectrometer. All the compounds were analyzed using a Waters Investigator Semiprep 15 SFC-MS instrument, confirming purity  $\geq 95\%$ .

##### 4.1.2. General procedure for the synthesis of 2-aminopyrrole analogues 2–30

The synthesis of 2-aminopyrrole analogues was based on a multicomponent reaction by refluxing a solution of three reactants including a methylsulfonamidoacetophenone, an aldehydes and a cyanoacetic acid with 0.6 equiv of  $\text{K}_2\text{CO}_3$  in ethanol. This reaction

results in three substituted 2-aminopyrroles [35]. Compounds **1–30** in Tables 1 and 2, and Fig. 3 were synthesized as shown in Scheme 1.

4.1.2.1. (5-Amino-4-(3,4-dichlorobenzoyl)-3-(2,4-dichlorophenyl)-1H-pyrrol-2-yl)(phenyl)methanone (**21B10**). 35% as yellow solid. Melting point (M.p.) 248–249  $^\circ\text{C}$ ;  $^1\text{H}$  NMR (500 MHz,  $\text{DMSO}-d_6$ )  $\delta$ : 11.31 (s, 1H), 7.31–7.22 (d,  $J = 8.0$  Hz, 2H), 7.24–7.21 (t,  $J = 7.5$  Hz, 1H), 7.20–7.18 (d,  $J = 7.5$  Hz, 2H), 7.10–6.91 (m, 7H), 6.84–6.75 (dd,  $J = 8.5, 2.5$  Hz, 2H).  $^{13}\text{C}$  NMR (126 MHz,  $\text{DMSO}-d_6$ )  $\delta$  189.19, 185.41, 151.71, 140.62, 138.92, 134.74, 134.17, 132.87, 132.74, 132.64, 130.79, 130.10, 129.85, 129.67, 128.24, 127.88, 127.86, 127.75, 127.63, 126.29, 122.57, 106.01. HRMS, calculated for  $\text{C}_{24}\text{H}_{14}\text{Cl}_4\text{N}_2\text{O}_2$   $[\text{M}+\text{H}]^+$ : 504.9890, found 504.9855.

4.1.2.2. (5-Amino-4-(4-chlorobenzoyl)-3-(2,4-dichlorophenyl)-1H-pyrrol-2-yl)(phenyl)methanone (**2**). 32% as yellow solid. M.p. 241–243  $^\circ\text{C}$ ;  $^1\text{H}$  NMR (500 MHz,  $\text{DMSO}-d_6$ )  $\delta$ : 11.28 (s, 1H), 7.22–7.16 (td,  $J = 7.5, 1.5$  Hz, 3H), 7.04–6.98 (m, 6H), 6.89 (d,  $J = 2.0$  Hz, 1H), 6.82 (s, 2H), 6.79–6.77 (d,  $J = 8.0$  Hz, 1H), 6.74–6.72 (dd,  $J = 6.0, 2.0$  Hz, 1H).  $^{13}\text{C}$  NMR (126 MHz,  $\text{DMSO}-d_6$ )  $\delta$  190.93, 185.32, 151.49, 139.05, 135.07, 134.70, 134.32, 132.85, 132.80, 130.68, 129.54, 128.21, 127.81, 127.60, 127.19, 126.09, 122.31, 106.18, 79.65, 72.94. HRMS, calculated for  $\text{C}_{24}\text{H}_{15}\text{Cl}_3\text{N}_2\text{O}_2$   $[\text{M}+\text{H}]^+$ : 469.0199, found 469.0262.

4.1.2.3. (5-Amino-4-(3-chlorobenzoyl)-3-(2,4-dichlorophenyl)-1H-pyrrol-2-yl)(phenyl)methanone (**3**). 31% as yellow solid. M.p. 225–227  $^\circ\text{C}$ ;  $^1\text{H}$  NMR (500 MHz,  $\text{DMSO}-d_6$ )  $\delta$ : 11.29 (s, 1H), 7.24–7.20 (td,  $J = 7.5, 1.5$  Hz, 1H), 7.17–7.17 (m, 3H), 7.08–7.02 (m, 4H), 6.93–6.92 (t,  $J = 1.5$  Hz, 1H), 6.89 (s, 2H), 6.88–6.87 (d,  $J = 2.5, 1\text{H}$ ) 6.84–6.82 (d,  $J = 8.3$  Hz, 1H), 6.73–6.71 (dd,  $J = 6.5, 2.5$  Hz, 1H).  $^{13}\text{C}$  NMR (126 MHz,  $\text{DMSO}-d_6$ )  $\delta$  190.31, 185.40, 151.68, 142.29, 138.96, 134.70, 134.19, 132.79, 132.70, 132.08, 130.71, 129.51, 129.50, 128.24, 128.01, 127.87, 127.60, 126.32, 122.45, 106.05. HRMS, calculated for  $\text{C}_{24}\text{H}_{15}\text{Cl}_3\text{N}_2\text{O}_2$   $[\text{M}+\text{H}]^+$ : 469.0199, found 469.0265.

4.1.2.4. (5-Amino-4-(3-bromobenzoyl)-3-(2,4-dichlorophenyl)-1H-pyrrol-2-yl)(phenyl)methanone (**4**). 25% as yellow solid. M.p. 260–262  $^\circ\text{C}$ ;  $^1\text{H}$  NMR (500 MHz,  $\text{DMSO}-d_6$ )  $\delta$ : 11.29 (s, 1H), 7.33–7.30 (ddd,  $J = 1.0, 1.0, 7.0$  Hz, 1H), 7.24–7.20 (td,  $J = 7.5, 1.5$  Hz, 1H), 7.19–7.17 (m, 2H), 7.14–7.12 (td,  $J = 7.5, 1.5$  Hz, 1H), 7.05–6.99 (m, 4H), 6.89–6.88 (d,  $J = 8.3$  Hz, 1H), 6.87 (s, 2H), 6.83–6.81 (dd,  $J = 8.5, 2.0$  Hz, 1H), 6.73–6.71 (dd,  $J = 6.5, 2.0$  Hz, 1H).  $^{13}\text{C}$  NMR (126 MHz,  $\text{DMSO}-d_6$ )  $\delta$  190.21, 185.40, 151.69, 142.51, 138.69, 134.64, 134.16, 132.76, 132.68, 132.42, 130.71, 130.32, 129.79, 128.26, 127.98, 127.92, 127.59, 126.68, 126.28, 122.47, 120.59, 106.02. HRMS, calculated for  $\text{C}_{24}\text{H}_{15}\text{BrCl}_2\text{N}_2\text{O}_2$   $[\text{M}+\text{H}]^+$ : 512.9694, found 512.9625.

4.1.2.5. (5-Amino-3-(2,4-dichlorophenyl)-4-(3-fluorobenzoyl)-1H-pyrrol-2-yl)(phenyl)methanone (**5**). 35% as yellow solid. M.p. 267–269  $^\circ\text{C}$ ;  $^1\text{H}$  NMR (500 MHz,  $\text{DMSO}-d_6$ )  $\delta$ : 11.29 (s, 1H), 7.25–7.20 (td,  $J = 7.5, 1.5$  Hz, 1H), 7.17–7.17 (m, 3H), 7.05–7.02 (m, 4H), 6.93–6.92 (t,  $J = 1.5$  Hz, 1H), 6.89 (s, 2H), 6.88–6.87 (d,  $J = 2.5, 1\text{H}$ ) 6.84–6.82 (dt,  $J = 8.5, 2.0$  Hz, 1H), 6.73–6.71 (dd,  $J = 6.5, 2.0$  Hz, 1H).  $^{13}\text{C}$  NMR (126 MHz,  $\text{DMSO}-d_6$ )  $\delta$  190.50, 185.37, 162.06, 160.11, 151.61, 142.75, 142.66, 138.88, 134.89, 134.28, 132.87, 132.68, 130.673, 129.56 (d,  $J = 9.2$  Hz), 128.21, 128.09, 127.80, 127.592, 126.03, 123.85, 122.41, 116.55 (d,  $J = 20.1$  Hz), 114.58 (d,  $J = 22.5$  Hz), 106.08. HRMS, calculated for  $\text{C}_{24}\text{H}_{15}\text{FCl}_2\text{N}_2\text{O}_2$   $[\text{M}+\text{H}]^+$ : 453.0495, found 453.0461.

4.1.2.6. (5-Amino-3-(2,4-dichlorophenyl)-4-(3-methylbenzoyl)-1H-pyrrol-2-yl)(phenyl)methanone (**6**). 40% as orange solid. M.p. 295–297  $^\circ\text{C}$ ;  $^1\text{H}$  NMR (500 MHz,  $\text{DMSO}-d_6$ )  $\delta$ : 11.24 (s, 1H),



7.22–7.19 (td,  $J = 7.5, 1.5$  Hz, 1H), 7.18–7.16 (m, 2H), 7.04–7.01 (t,  $J = 7.5$  Hz, 2H), 7.00–6.93 (m, 3H), 6.85 (d,  $J = 2.0$  Hz, 1H), 6.80 (d,  $J = 2.0$  Hz, 2H), 6.78 (s, 1H), 6.70–6.68 (dd,  $J = 6.5, 2.0$  Hz, 1H), 1.97 (s, 3H).  $^{13}\text{C}$  NMR (126 MHz, DMSO- $d_6$ )  $\delta$  192.40, 185.27, 151.41, 140.38, 139.06, 136.10, 134.70, 134.22, 133.11, 132.39, 130.60, 130.34, 128.60, 128.36, 128.29, 127.68, 127.60, 127.54, 125.94, 124.91, 122.13, 106.39, 20.81. HRMS, calculated for  $\text{C}_{25}\text{H}_{17}\text{Cl}_2\text{N}_2\text{O}_2$   $[\text{M}+\text{H}]^+$ : 449.0745, found 449.0816.

4.1.2.7. (5-Amino-3-(2,4-dichlorophenyl)-1H-pyrrole-2,4-diyl) bis(phenylmethanone) (**7**). 37% as yellow solid. M.p. 267–269 °C;  $^1\text{H}$  NMR (500 MHz, DMSO- $d_6$ )  $\delta$ : 11.26 (s, 1H), 7.22–7.21 (t,  $J = 7.5$  Hz, 1H), 7.20–7.12 (m, 3H), 7.06–7.00 (m, 4H), 6.97–6.94 (m,  $J = 7.6$  Hz, 2H), 6.82–6.78 (m, 4H), 6.69–6.68 (dd,  $J = 8.0, 2.0$  Hz, 1H).  $^{13}\text{C}$  NMR (126 MHz, DMSO- $d_6$ )  $\delta$  192.31, 185.28, 151.41, 140.43, 139.10, 135.00, 134.31, 132.98, 132.51, 130.58, 129.79, 128.38, 128.23, 127.79, 127.56, 127.20, 125.96, 122.18, 106.36, 99.98. HRMS, calculated for  $\text{C}_{24}\text{H}_{16}\text{Cl}_2\text{N}_2\text{O}_2$   $[\text{M}+\text{H}]^+$ : 435.0589, found 435.0570.

4.1.2.8. (5-Amino-3-(2,4-dichlorophenyl)-4-(thiophene-2-carbonyl)-1H-pyrrol-2-yl)(phenyl)methanone (**8**). 45% as yellow solid. M.p. 244–246 °C;  $^1\text{H}$  NMR (500 MHz, DMSO- $d_6$ )  $\delta$ : 11.25 (s, 1H), 7.58 (d,  $J = 7.0$  Hz, 1H), 7.24 (d,  $J = 8.0$  Hz, 1H), 7.19 (d,  $J = 7.5$  Hz, 1H), 7.08–7.04 (m, 3H), 6.95 (d,  $J = 8.5$  Hz, 1H), 6.83 (d,  $J = 8.5$  Hz, 1H), 6.69 (d,  $J = 2.0$  Hz, 1H), 6.61–6.56 (m, 1H), 6.54 (s, 2H).  $^{13}\text{C}$  NMR (126 MHz, DMSO- $d_6$ )  $\delta$  193.31, 185.24, 151.42, 141.43, 139.10, 135.31, 132.98, 133.51, 130.58, 129.74, 128.38, 128.23, 127.74, 127.52, 127.21, 123.18, 105.36, 99.92. HRMS, calculated for  $\text{C}_{22}\text{H}_{14}\text{Cl}_2\text{N}_2\text{O}_2\text{S}$   $[\text{M}+\text{H}]^+$ : 441.0153, found 441.1923.

4.1.2.9. 2-Amino-5-benzoyl-4-(2,4-dichlorophenyl)-1H-pyrrole-3-carboxamide (**9**). 35% as yellow solid. M.p. 210–212 °C;  $^1\text{H}$  NMR (500 MHz, DMSO- $d_6$ )  $\delta$ : 11.05 (s, 1H), 7.30 (s, 1H), 7.24 (d,  $J = 8.0$  Hz, 1H), 7.26–7.21 (m, 2H), 7.18–7.16 (m, 2H), 7.13 (s, 2H), 7.12–7.02 (m, 3H), 6.35 (s, 2H).  $^{13}\text{C}$  NMR (126 MHz, DMSO- $d_6$ )  $\delta$  183.98, 167.24, 149.74, 139.68, 134.97, 134.37, 133.89, 132.70, 130.01, 129.09, 127.69, 127.63, 127.35, 123.85, 121.33, 99.60. HRMS, calculated for  $\text{C}_{18}\text{H}_{13}\text{Cl}_2\text{N}_3\text{O}_2$   $[\text{M}+\text{H}]^+$ : 374.0385, found 374.0322.

4.1.2.10. (5-Amino-4-(3,4-dichlorobenzoyl)-1H-pyrrol-2-yl)(phenyl)methanone (**10**). 15% as yellow solid. M.p. 223–225 °C;  $^1\text{H}$  NMR (500 MHz, DMSO- $d_6$ )  $\delta$ : 10.84 (s, 1H), 7.91–7.85 (d,  $J = 7.5$  Hz, 1H), 7.83–7.74 (m, 2H), 7.66–7.63 (td,  $J = 7.5, 1.5$  Hz, 1H), 7.60–7.48 (m, 5H), 6.97 (d,  $J = 2.4$  Hz, 1H), 6.68 (s, 2H).  $^{13}\text{C}$  NMR (126 MHz, DMSO- $d_6$ )  $\delta$  187.83, 182.68, 152.68, 142.30, 138.69, 133.75, 131.93, 131.14, 130.85, 128.90, 128.69, 127.94, 126.98, 124.262, 122.08. HRMS, calculated for  $\text{C}_{18}\text{H}_{12}\text{Cl}_2\text{N}_2\text{O}_2$   $[\text{M}+\text{H}]^+$ : 359.0276, found 359.0223.

4.1.2.11. (5-Amino-4-(3,4-dichlorobenzoyl)-3-(naphthalen-1-yl)-1H-pyrrol-2-yl)(phenyl)methanone (**11**). 23% as yellow solid. M.p. 297–299 °C;  $^1\text{H}$  NMR (500 MHz, DMSO- $d_6$ )  $\delta$ : 11.28 (s, 1H), 7.61 (d,  $J = 8.3$  Hz, 1H), 7.53 (d,  $J = 8.0$  Hz, 1H), 7.39–7.35 (m, 1H), 7.32 (dt,  $J = 8.0, 5.0$  Hz, 2H), 7.00–6.97 (dd,  $J = 7.0, 2.0$  Hz, 2H), 6.96–6.90 (m, 3H), 6.85–6.81 (m, 2H), 6.74 (d,  $J = 2.0$  Hz, 1H), 6.67 (d,  $J = 8.0$  Hz, 1H), 6.63–6.57 (m, 3H).  $^{13}\text{C}$  NMR (126 MHz, DMSO- $d_6$ )  $\delta$  189.97, 185.73, 151.86, 140.38, 139.20, 132.64, 132.55, 131.97, 131.59, 130.86, 130.38, 130.03, 129.40, 128.54, 128.23, 127.83, 127.69, 127.29, 126.96, 126.55, 126.32, 125.71, 124.63, 123.16, 107.34. HRMS, calculated for  $\text{C}_{28}\text{H}_{18}\text{Cl}_2\text{N}_2\text{O}_2$   $[\text{M}+\text{H}]^+$ : 485.0745, found 485.0819.

4.1.2.12. (5-Amino-4-(3,4-dichlorobenzoyl)-3-(naphthalen-2-yl)-1H-pyrrol-2-yl)(phenyl)methanone (**12**). 32% as yellow solid. M.p. 248–249 °C;  $^1\text{H}$  NMR (500 MHz, DMSO- $d_6$ )  $\delta$ : 11.19 (s, 1H), 7.58 (d,  $J = 8.0$  Hz, 1H), 7.40 (d,  $J = 8.5$  Hz, 1H), 7.34–7.27 (m, 2H), 7.21–7.15 (m, 4H), 7.04 (d,  $J = 2.0$  Hz, 1H), 6.98 (dd,  $J = 8.5, 2.0$  Hz, 1H),

6.94–6.89 (m, 2H), 6.88 (d,  $J = 1.5$  Hz, 2H), 6.80 (t,  $J = 7.5$  Hz, 2H), 6.74 (dd,  $J = 8.5, 2.0$  Hz, 1H).  $^{13}\text{C}$  NMR (126 MHz, DMSO- $d_6$ )  $\delta$  189.65, 185.66, 151.70, 140.90, 139.15, 133.33, 132.18, 132.14, 131.51, 131.23, 130.88, 130.43, 130.17, 129.77, 129.45, 128.78, 128.58, 127.65, 127.65, 127.63, 127.45, 127.32, 126.24, 126.15, 125.81, 122.18, 106.77. HRMS, calculated for  $\text{C}_{28}\text{H}_{18}\text{Cl}_2\text{N}_2\text{O}_2$   $[\text{M}+\text{H}]^+$ : 485.0745, found 485.0816.

4.1.2.13. (5-Amino-4-(3,4-dichlorobenzoyl)-3-(2,6-difluorophenyl)-1H-pyrrol-2-yl)(phenyl)methanone (**13**). 33% as yellow solid. M.p. 257–259 °C;  $^1\text{H}$  NMR (500 MHz, DMSO- $d_6$ )  $\delta$ : 11.42 (s, 1H), 7.31–7.29 (d,  $J = 8.0$  Hz, 1H), 7.23–7.21 (m, 3H), 7.15 (s, 1H), 7.10–7.05 (q,  $J = 8.5$  Hz, 3H), 6.94–6.91 (m, 1H), 6.88 (s, 2H), 6.43 (t,  $J = 8.0$  Hz, 2H).  $^{13}\text{C}$  NMR (126 MHz, DMSO- $d_6$ )  $\delta$  188.95, 185.48, 160.01 (d,  $J = 6.5$  Hz), 158.08 (d,  $J = 6.8$  Hz), 151.86, 140.44, 138.57, 132.84, 131.31 (m), 130.34, 130.11, 129.32, 127.96, 127.73, 127.28, 127.87, 117.56, 110.96 (d,  $J = 3.3$  Hz), 110.78 (d,  $J = 2.9$  Hz), 105.61. HRMS, calculated for  $\text{C}_{24}\text{H}_{14}\text{Cl}_2\text{F}_2\text{N}_2\text{O}_2$   $[\text{M}+\text{H}]^+$ : 471.0400, found 471.0389.

4.1.2.14. (5-Amino-4-(3-chlorobenzoyl)-1H-pyrrol-2-yl)(phenyl)methanone (**14**). 31% as yellow solid. M.p. 231–233 °C;  $^1\text{H}$  NMR (500 MHz, DMSO- $d_6$ )  $\delta$ : 11.20 (s, 1H), 7.76–7.73 (m, 2H), 7.67–7.63 (m, 2H), 7.62–7.55 (m, 2H), 7.50 (dt,  $J = 8.5, 7.5$  Hz, 3H), 6.93 (s, 2H), 6.70 (d,  $J = 2.5$  Hz, 1H).  $^{13}\text{C}$  NMR (126 MHz, DMSO- $d_6$ )  $\delta$  187.83, 182.69, 152.69, 142.30, 138.70, 133.76, 131.94, 130.86, 128.90, 128.70, 127.90, 126.98, 124.26, 122.08, 105.98. HRMS, calculated for  $\text{C}_{18}\text{H}_{13}\text{Cl}_1\text{N}_2\text{O}_2$   $[\text{M}+\text{H}]^+$ : 325.066, found 325.069.

4.1.2.15. (4-([1,1'-biphenyl]-4-yl)-2-amino-5-benzoyl-1H-pyrrol-3-yl)(3-chlorophenyl)methanone (**15**). 32% as yellow solid. M.p. 211–213 °C;  $^1\text{H}$  NMR (500 MHz, DMSO- $d_6$ )  $\delta$ : 11.16 (s, 1H), 7.44–7.39 (m, 2H), 7.34–7.29 (m, 3H), 7.20–7.15 (m, 2H), 7.14–7.06 (m, 2H), 7.06–7.02 (m, 1H), 7.01–6.90 (m, 4H), 6.87 (s, 2H), 6.85–6.81 (d,  $J = 8.5$  Hz, 1H), 6.69–6.64 (d,  $J = 8.5$  Hz, 2H).  $^{13}\text{C}$  NMR (126 MHz, DMSO- $d_6$ )  $\delta$  190.63, 185.56, 151.71, 142.49, 140.47, 139.23, 138.38, 133.30, 133.16, 132.19, 131.59, 130.25, 129.51, 129.33, 129.26, 128.66, 128.19, 127.59, 127.55, 126.82, 126.59, 125.25, 122.10, 106.53. HRMS, calculated for  $\text{C}_{30}\text{H}_{21}\text{Cl}_1\text{N}_2\text{O}_2$   $[\text{M}+\text{H}]^+$ : 477.1292, found 477.1361.

4.1.2.16. (5-Amino-4-(3-chlorobenzoyl)-3-phenyl-1H-pyrrol-2-yl)(phenyl)methanone (**16**). 35% as yellow solid. M.p. 264–265 °C;  $^1\text{H}$  NMR (500 MHz, DMSO- $d_6$ )  $\delta$ : 11.12 (s, 1H), 7.15–7.07 (m, 4H), 7.02 (dt,  $J = 7.5, 2.0$  Hz, 1H), 6.96–6.92 (m, 4H), 6.81 (s, 2H), 6.72 (td,  $J = 6.5, 2.5$  Hz, 1H), 6.64 (m, 4H).  $^{13}\text{C}$  NMR (126 MHz, DMSO- $d_6$ )  $\delta$  190.62, 185.62, 151.60, 142.45, 139.13, 133.93, 133.46, 132.20, 131.17, 130.44, 129.59, 129.40, 128.62, 128.12, 127.52, 126.89, 126.60, 126.57, 122.01, 106.46. HRMS, calculated for  $\text{C}_{30}\text{H}_{21}\text{Cl}_1\text{N}_2\text{O}_2$   $[\text{M}+\text{H}]^+$ : 401.0979, found 401.1051.

4.1.2.17. (5-Amino-4-(3-chlorobenzoyl)-3-(3,4-dichlorophenyl)-1H-pyrrol-2-yl)(phenyl)methanone (**17**). 32% as yellow solid. M.p. 253–255 °C;  $^1\text{H}$  NMR (500 MHz, DMSO- $d_6$ )  $\delta$ : 11.25 (s, 1H), 7.22–7.20 (td,  $J = 7.5, 2.0$  Hz, 1H), 7.19–7.15 (m, 3H), 7.07–7.01 (m, 4H), 6.94–6.92 (m, 1H), 6.89 (s, 2H), 6.84–6.80 (d,  $J = 2.0, 2.0$  Hz), 6.57 (dd,  $J = 8.5, 2.0$  Hz, 1H).  $^{13}\text{C}$  NMR (126 MHz, DMSO- $d_6$ )  $\delta$  190.29, 185.46, 151.61, 142.48, 139.16, 134.82, 133.04, 132.94, 132.49, 131.06, 130.60, 130.02, 129.63, 129.48, 129.41, 128.72, 128.50, 127.88, 127.69, 126.43, 122.36, 106.44. HRMS, calculated for  $\text{C}_{24}\text{H}_{15}\text{Cl}_3\text{N}_2\text{O}_2$   $[\text{M}+\text{H}]^+$ : 469.0199, found 469.0274.

4.1.2.18. (5-Amino-4-(3-chlorobenzoyl)-3-(4-chlorophenyl)-1H-pyrrol-2-yl)(phenyl)methanone (**18**). 25% as yellow solid. M.p. 248–249 °C;  $^1\text{H}$  NMR (500 MHz, DMSO- $d_6$ )  $\delta$ : 11.18 (s, 1H), 7.22–7.19 (td,  $J = 7.5, 2.0$  Hz, 1H), 7.16–7.13 (m, 2H), 7.05–6.98 (m,

4H), 6.91 (t,  $J = 2.0$  Hz, 1H), 6.85 (s, 2H), 6.63 (m, 4H).  $^{13}\text{C}$  NMR (126 MHz, DMSO- $d_6$ )  $\delta$  190.41, 185.52, 151.63, 142.44, 139.12, 133.00, 132.70, 132.30, 132.06, 131.51, 130.51, 129.60, 129.51, 128.67, 128.12, 127.66, 126.76, 126.64, 122.16, 106.47. MS (ESI): HRMS, calculated for  $\text{C}_{24}\text{H}_{16}\text{Cl}_2\text{N}_2\text{O}_2$   $[\text{M}+\text{H}]^+$ : 435.0589, found 435.0661.

4.1.2.19. (5-Amino-4-(3-chlorobenzoyl)-3-(2-chlorophenyl)-1H-pyrrol-2-yl)(phenyl)methanone (**19**). 32% as yellow solid. M.p. 289–285 °C;  $^1\text{H}$  NMR (500 MHz, DMSO- $d_6$ )  $\delta$ : 11.23 (s, 1H), 7.19–7.15 (m, 2H), 7.13 (dt,  $J = 7.5, 2.0$  Hz, 1H), 7.10 (ddd,  $J = 8.0, 2.5, 1.0$  Hz, 1H), 7.05 (dt,  $J = 7.5, 1.5$  Hz, 1H), 7.00–6.98 (m, 1H), 6.97–6.95 (m, 2H), 6.85 (s, 2H), 6.80 (dt,  $J = 7.5, 1.0$  Hz, 1H), 6.79–6.74 (m, 2H), 6.69–6.64 (m, 1H).  $^{13}\text{C}$  NMR (126 MHz, DMSO- $d_6$ )  $\delta$  190.51, 185.51, 151.62, 142.29, 138.94, 133.61, 133.57, 133.33, 132.02, 130.65, 129.61, 129.72, 129.14, 128.90, 128.49, 128.25, 127.58, 127.47, 126.29, 126.05, 122.34, 106.08. HRMS, calculated for  $\text{C}_{24}\text{H}_{16}\text{Cl}_2\text{N}_2\text{O}_2$   $[\text{M}+\text{H}]^+$ : 435.0589, found 435.0660.

4.1.2.20. (5-Amino-4-(3-chlorobenzoyl)-3-(3-chlorophenyl)-1H-pyrrol-2-yl)(phenyl)methanone (**20**). 36% as yellow solid. M.p. 258–260 °C;  $^1\text{H}$  NMR (500 MHz, DMSO- $d_6$ )  $\delta$ : 11.21 (s, 1H), 7.22–7.11 (m, 4H), 7.06–6.95 (m, 5H), 6.85 (s, 2H), 6.77 (dt,  $J = 8.0, 1.5$  Hz, 1H), 6.65 (d,  $J = 2.0$  Hz, 1H), 6.62 (t,  $J = 7.5$  Hz, 1H), 6.56 (dt,  $J = 7.5, 1.5$  Hz, 1H).  $^{13}\text{C}$  NMR (126 MHz, DMSO- $d_6$ )  $\delta$  190.43, 185.54, 151.57, 142.46, 139.39, 136.07, 132.45, 132.08, 131.77, 131.01, 130.65, 129.70, 129.66, 129.48, 128.49, 128.46, 127.88, 127.61, 126.45, 126.39, 122.22, 106.39. HRMS, calculated for  $\text{C}_{24}\text{H}_{16}\text{Cl}_2\text{N}_2\text{O}_2$   $[\text{M}+\text{H}]^+$ : 435.0589, found 435.0661.

4.1.2.21. (5-Amino-4-(3-chlorobenzoyl)-3-(2,4-difluorophenyl)-1H-pyrrol-2-yl)(phenyl)methanone (**21**). 34% as yellow solid. M.p. 257–259 °C;  $^1\text{H}$  NMR (500 MHz, DMSO- $d_6$ )  $\delta$ : 11.29 (s, 1H), 7.25–7.15 (m, 4H), 7.07–7.03 (m, 4H), 6.97–6.95 (m, 1H), 6.85 (s, 2H), 6.77–6.72 (qd,  $J = 8.5, 6.5$  Hz, 1H), 6.46–6.44 (td,  $J = 8.5, 2.5$  Hz, 1H), 6.38–6.36 (td,  $J = 8.5, 2.5$  Hz, 1H).  $^{13}\text{C}$  NMR (126 MHz, DMSO- $d_6$ )  $\delta$  190.27, 185.46, 160.98 (d,  $J = 7.0$  Hz), 160.96 (d,  $J = 6.5$  Hz), 157.96, 157.95, 151.69, 142.22, 138.90, 134.12 (d,  $J = 7.5$  Hz), 134.04 (d,  $J = 7.5$  Hz), 132.26, 130.76, 129.72, 129.62, 128.29, 127.68, 127.66, 126.30, 124.70, 122.62, 110.61 (d,  $J = 2.6$  Hz), 110.46 (d,  $J = 2.7$  Hz), 106.20, 103.30, 102.82 (t,  $J = 25.6$  Hz), 102.61, 99.98. HRMS, calculated for  $\text{C}_{24}\text{H}_{15}\text{Cl}_1\text{F}_2\text{N}_2\text{O}_2$   $[\text{M}+\text{H}]^+$ : 437.0790, found 437.0861.

4.1.2.22. (5-Amino-4-(3-chlorobenzoyl)-3-(2,4-dihydroxyphenyl)-1H-pyrrol-2-yl)(phenyl)methanone (**22**). 22% as brown solid. M.p. 243–245 °C;  $^1\text{H}$  NMR (500 MHz, DMSO- $d_6$ )  $\delta$ : 10.89 (s, 1H), 8.75 (s, 1H), 8.72 (s, 1H), 7.22–7.19 (m, 2H), 7.18–7.12 (m, 2H), 7.05 (t,  $J = 2.0$  Hz, 1H), 7.03–7.01 (dt,  $J = 7.5, 2.0$  Hz, 1H), 7.00–6.93 (m, 3H), 6.68 (s, 2H), 6.17 (d,  $J = 8.0$  Hz, 1H), 5.60 (d,  $J = 2.5$  Hz, 1H), 5.53 (dd,  $J = 8.0, 2.5$  Hz, 1H).  $^{13}\text{C}$  NMR (126 MHz, DMSO- $d_6$ )  $\delta$  191.10, 185.55, 157.91, 155.55, 151.50, 142.45, 139.33, 132.70, 131.83, 130.63, 130.25, 129.32, 128.62, 128.55, 128.01, 127.16, 126.72, 121.83, 112.81, 106.42, 105.93, 101.67. HRMS, calculated for  $\text{C}_{24}\text{H}_{17}\text{Cl}_1\text{N}_2\text{O}_4$   $[\text{M}+\text{H}]^+$ : 433.0877, found 433.0875.

4.1.2.23. (5-Amino-4-(3-chlorobenzoyl)-3-(2,4-dimethylphenyl)-1H-pyrrol-2-yl)(phenyl)methanone (**23**). 45% as orange solid. M.p. 267–269 °C;  $^1\text{H}$  NMR (500 MHz, DMSO- $d_6$ )  $\delta$ : 11.05 (s, 1H), 7.16–7.07 (m, 4H), 7.04–6.92 (m, 4H), 6.86 (s, 2H), 6.81 (d,  $J = 2.0$  Hz, 1H), 6.48–6.44 (m, 1H), 6.32 (d,  $J = 6.5$  Hz, 2H), 1.94 (s, 3H), 1.83 (s, 3H).  $^{13}\text{C}$  NMR (126 MHz, DMSO- $d_6$ )  $\delta$  190.91, 185.52, 151.89, 142.39, 139.05, 136.07, 135.62, 132.33, 131.89, 131.75, 130.99, 130.28, 129.64, 129.20, 129.10, 128.22, 127.50, 127.31, 126.06, 125.43, 122.20, 106.58, 20.92, 20.37. HRMS, calculated for  $\text{C}_{26}\text{H}_{21}\text{Cl}_1\text{N}_2\text{O}_2$   $[\text{M}+\text{H}]^+$ : 429.1295, found 429.1291.

4.1.2.24. (5-Amino-3-(benzo[d][1,3]dioxol-5-yl)-4-(3-chlorobenzoyl)-1H-pyrrol-2-yl)(phenyl)methanone (**24**). 27% as yellow solid. M.p. 255–257 °C;  $^1\text{H}$  NMR (500 MHz, DMSO- $d_6$ )  $\delta$ : 11.07 (s, 1H), 7.22–7.16 (m, 4H), 7.06–7.00 (m, 4H), 6.95 (t,  $J = 2.0$  Hz, 1H), 6.83 (s, 2H), 6.16–6.15 (t,  $J = 2.0$  Hz, 1H), 6.13 (s, 1H), 6.06–6.05 (dd,  $J = 8.0, 2.0$  Hz, 1H), 5.69 (s, 2H).  $^{13}\text{C}$  NMR (126 MHz, DMSO- $d_6$ )  $\delta$  190.62, 185.50, 151.59, 146.34, 146.01, 142.67, 139.40, 133.31, 132.25, 130.36, 129.45, 129.43, 128.52, 127.89, 127.69, 127.52, 126.46, 125.16, 122.03, 111.55, 107.02, 106.55, 100.87. HRMS, calculated for  $\text{C}_{25}\text{H}_{17}\text{Cl}_1\text{N}_2\text{O}_2$   $[\text{M}+\text{H}]^+$ : 445.0877, found 445.0947.

4.1.2.25. (5-Amino-4-(3-chlorobenzoyl)-3-(pyridin-4-yl)-1H-pyrrol-2-yl)(phenyl)methanone (**25**). 35% as yellow solid. M.p. 250–252 °C;  $^1\text{H}$  NMR (500 MHz, DMSO- $d_6$ )  $\delta$ : 11.30 (s, 1H), 7.79–7.75 (dd,  $J = 2.5, 2.0, 2\text{H}$ ), 7.23–7.13 (m, 4H), 7.06 (dt,  $J = 7.5, 1.5$  Hz, 1H), 7.03–6.97 (m, 4H), 6.85 (s, 2H), 6.65–6.59 (dd,  $J = 2.5, 2.0, 2\text{H}$ ).  $^{13}\text{C}$  NMR (126 MHz, DMSO- $d_6$ )  $\delta$  190.22, 185.55, 151.58, 147.81, 142.39, 142.35, 139.01, 132.34, 130.96, 130.38, 129.92, 129.67, 128.64, 128.14, 127.76, 126.64, 126.08, 122.26, 106.16. HRMS, calculated for  $\text{C}_{23}\text{H}_{16}\text{Cl}_1\text{N}_3\text{O}_2$   $[\text{M}+\text{H}]^+$ : 402.0931, found 402.1003.

4.1.2.26. (5-Amino-4-(3-chlorobenzoyl)-3-(pyridin-3-yl)-1H-pyrrol-2-yl)(phenyl)methanone (**26**). 35% as yellow solid. M.p. 242–244 °C;  $^1\text{H}$  NMR (500 MHz, DMSO- $d_6$ )  $\delta$ : 11.27 (s, 1H), 7.89–7.88 (dd,  $J = 5.0, 2.0$  Hz, 1H), 7.79 (dd,  $J = 2.0, 1.0$  Hz, 1H), 7.16 (ddd,  $J = 8.0, 2.0, 1.0$  Hz, 3H), 7.14–7.11 (m, 1H), 7.05–6.94 (m, 6H), 6.86 (s, 2H), 6.63–6.62 (ddd,  $J = 7.5, 5.0, 1.0$  Hz, 1H).  $^{13}\text{C}$  NMR (126 MHz, DMSO- $d_6$ )  $\delta$  190.29, 185.46, 151.70, 150.90, 147.18, 142.35, 138.92, 137.46, 130.72, 130.22, 129.74, 129.65, 129.59, 128.71, 128.08, 127.78, 126.72, 122.67, 121.78, 106.63. HRMS, calculated for  $\text{C}_{23}\text{H}_{16}\text{Cl}_1\text{N}_3\text{O}_2$   $[\text{M}+\text{H}]^+$ : 402.0931, found 402.1001.

4.1.2.27. (5-Amino-4-(3-chlorobenzoyl)-3-(2,4-dimethoxyphenyl)-1H-pyrrol-2-yl)(phenyl)methanone (**27**). 32% as yellow solid. M.p. 235–237 °C;  $^1\text{H}$  NMR (500 MHz, DMSO- $d_6$ )  $\delta$ : 11.00 (s, 1H), 7.15–7.10 (m, 4H), 7.03–6.93 (m, 4H), 6.89 (q,  $J = 1.0$  Hz, 1H), 6.76 (s, 2H), 6.42 (d,  $J = 8.0$  Hz, 1H), 5.87–5.85 (dd,  $J = 6.0, 2.0$  Hz, 1H), 5.73–5.72 (d,  $J = 2.5$  Hz, 1H), 3.51 (s, 3H), 3.36 (s, 3H).  $^{13}\text{C}$  NMR (126 MHz, DMSO- $d_6$ )  $\delta$  190.78, 185.56, 160.36, 157.09, 151.65, 142.38, 139.16, 132.68, 131.82, 130.31, 129.59, 129.35, 129.02, 128.19, 127.60, 127.19, 122.08, 115.98, 106.29, 104.44, 97.30, 55.56, 54.81. HRMS, calculated for  $\text{C}_{26}\text{H}_{21}\text{Cl}_1\text{N}_2\text{O}_2$   $[\text{M}+\text{H}]^+$ : 461.1190, found 461.1236.

4.1.2.28. Ethyl 1H-pyrrole-2-carboxylate (**28**). White solid. M.p. 130–132 °C;  $^1\text{H}$  NMR (500 MHz, DMSO- $d_6$ )  $\delta$ : 9.26 (s, 1H), 6.98 (td,  $J = 2.5, 1.5$  Hz, 1H), 6.95 (ddd,  $J = 4.0, 2.5, 1.5$  Hz, 1H), 6.29 (dt,  $J = 4.0, 2.5$  Hz, 1H), 4.35 (q,  $J = 7.0$  Hz, 2H), 1.39 (t,  $J = 7.0$  Hz, 3H).  $^{13}\text{C}$  NMR (126 MHz, DMSO- $d_6$ )  $\delta$  161.22, 123.01, 122.68, 115.08, 110.40, 60.32, 14.47. HRMS, calculated for  $\text{C}_7\text{H}_9\text{N}_1\text{O}_2$   $[\text{M}+\text{H}]^+$ : 140.0633, found 140.0599.

4.1.2.29. Ethyl 5-amino-1H-pyrrole-2-carboxylate (**29**). Purple oil.  $^1\text{H}$  NMR (500 MHz, DMSO- $d_6$ )  $\delta$ : 8.83 (s, 1H), 6.53 (t,  $J = 2.5$  Hz, 1H), 6.50 (d,  $J = 2.5$  Hz, 1H), 4.31 (q,  $J = 7.0$  Hz, 2H), 1.36 (t,  $J = 7.0$  Hz, 3H).  $^{13}\text{C}$  NMR (126 MHz, DMSO- $d_6$ )  $\delta$  160.78, 134.75, 110.39, 105.27, 59.51, 14.49. HRMS, calculated for  $\text{C}_7\text{H}_{10}\text{N}_2\text{O}_2$   $[\text{M}+\text{H}]^+$ : 155.0742, found 155.0715.

4.1.2.30. (5-Amino-4-(3-chlorobenzoyl)-3-(2,4-dichlorophenyl)-1H-pyrrol-2-yl)(4-chlorophenyl)methanone (**30**). 38% as yellow solid. M.p. 273–275 °C;  $^1\text{H}$  NMR (500 MHz, DMSO- $d_6$ )  $\delta$ : 11.34 (s, 1H), 7.19–7.18 (dt,  $J = 7.0, 2.0$  Hz, 1H), 7.17–7.14 (m, 2H), 7.10–7.06 (m, 4H), 6.94 (d,  $J = 2.0$  Hz, 2H), 6.90 (s, 2H), 6.83 (d,  $J = 8.0$  Hz, 1H), 6.78–6.77 (dd,  $J = 8.0, 2.0$  Hz, 1H).  $^{13}\text{C}$  NMR (126 MHz, DMSO- $d_6$ )  $\delta$  190.32, 184.06, 165.92, 151.80, 142.24, 137.71, 135.54, 134.75,

134.18, 132.96, 132.62, 132.12, 129.99, 129.58, 129.56, 128.50, 127.95, 127.94, 127.61, 127.52, 126.30, 122.37, 106.18, 40.49, 40.41, 40.32, 40.25, 40.16, 40.08, 39.99, 39.91, 39.82, 39.66, 39.49. HRMS, calculated for  $C_{24}H_{14}Cl_2N_2O_2$   $[M+H]^+$ : 502.9809, found 502.9779.

#### 4.1.3. Human 15-LOX-1 enzyme inhibition studies

The h-15-LOX-1 enzyme activity studies were done using procedures previously described by our group [27,42]. h-15-LOX-1 was expressed and purified as described previously. h-15-LOX-1 activity was determined by the conversion of linoleic acid to 13S-hydroperoxy-9Z, 11E-octadecadienoic acid (13(S)-HpODE) ( $\lambda_{max}$  of 234 nm) in a 96-well plate. The conversion rate was followed by UV absorbance at 234 nm over time. The conversion rate was evaluated at the linear part of the plot, before substrate depletion covers the first 16 min of the reaction under the applied conditions. The optimum concentration of h-15-LOX-1 was determined by an enzyme activity assay and proved to be a 100-fold dilution. The absorbance increased at 234 nm over time for the conversion of linoleic acid in the presence (positive control) of the enzyme, or remained constant in the absence (blank control) of the enzyme.

The assay buffer consists of 25 mM HEPES titrated to pH 7.4 using a concentrated aqueous solution of 1 M NaOH. The substrate, linoleic acid (LA) (Sigma-Aldrich, L1376), was dissolved in ethanol to a concentration of 500  $\mu$ M. The inhibitor stock solution (10 mM in DMSO) was diluted with assay buffer to 71.4  $\mu$ M prepared for the SOS. 140  $\mu$ L of this solution were mixed with 50  $\mu$ L of 1:100 enzyme solution and incubated for 10 min at room temperature. After incubation, 10  $\mu$ L of 500  $\mu$ M LA was added to the mixture, which resulted in a mixture with 50  $\mu$ M inhibitor, a final dilution of the enzyme of 1:400 and 25  $\mu$ M LA. The linear absorbance increased in the absence of the inhibitor was set to 100%, whereas the absorbance increased in the absence of the enzyme was set to 0%. All experiments were performed in triplicate, and the average triplicate values and their standard deviations were plotted. The half-maximal inhibition concentration ( $IC_{50}$ ) of the inhibitors for h-15-LOX-1 were determined using the same assay. Briefly, the inhibitors were diluted with assay buffer. Using a serial dilution, the desired concentrations of the inhibitor were obtained, ranging from 0.39 to 200  $\mu$ M or 0.19–100  $\mu$ M, depending on the inhibitory potency and solubility of different inhibitors in water with 0%–5% DMSO. Data analysis was performed using Microsoft Excel professional plus 2013 and GraphPad Prism 5.01.

#### 4.1.4. Neutral red assay for quantitation of hepatocarcinoma HCC cells

HCC-1.2 human hepatocarcinoma cells (Kind gift of Prof. Bettina Grasl-Kraupp) were cultured in RPMI1640 medium containing 10% heat inactivated foetal calf serum (FCS). The cells were kept under standard tissue culture conditions at 37 °C, 5%CO<sub>2</sub> and 95% humidity and regularly checked for mycoplasma contaminations.  $2 \times 10^5$  cells/well were seeded into 24 well plates and grown for 48 h. To quantify viable cells, neutral red (50  $\mu$ g/mL) uptake from serum-free medium during 2 h of incubation was measured in triplicate wells in each experiment. The dye was taken up into the lysosomes of viable cells and dissolved with 1% acetic acid in 70% ethanol. The absorption difference between 560 nm and 620 nm was measured using an Anthos Plate Reader. The results of three to five independent experiments are summarized.

#### 4.1.5. Photoactivation study

To perform light sensitivity screening against h-15-LOX-1 on UV assay, all experiments have been performed in triplicate under the day light irradiation, 365 nm UV irradiation and darkness with same concentration of inhibitor depending on the inhibitory potency. H-15-LOX-1 was then incubated with inhibitor medium for 2,

5 and 10 min. Afterwards, enzyme activity was followed by measuring UV absorbance of 13(S)-HpODE at 234 nm over 16 min according to positive control without inhibitor. To verify light sensitivity on cytotoxicity experiment, we have performed pilot cytotoxicity experiments in HCC-1.2 cell line with selected h-15-LOX-1 inhibitors under day light and, in turn, incubated cells either upon irradiation with UV-light for 10 min or protected the cells from light. All experiments were repeated at least twice.

#### Acknowledgements

We acknowledge The Netherlands Organisation for Scientific Research (NWO) for providing a VIDI grant (016.122.302) to F.J.D. and Mrs. Martha Seif for her excellent technical assistance in cell culture experiments.

#### Appendix A. Supplementary data

Supplementary data related to this article can be found at <http://dx.doi.org/10.1016/j.ejmech.2017.07.047>.

#### References

- [1] S. Rakoff-Nahoum, Why cancer and inflammation? *Yale J. Biol. Med.* 79 (2006) 123–130.
- [2] S.I. Grivennikov, F.R. Greten, M. Karin, Immunity, Inflammation, and Cancer Cell, vol. 140, 2011, pp. 883–899.
- [3] A. Ahmad, S. Banerjee, Z. Wang, D. Kong, A.P.N. Majumdar, F.H. Sarkar, Aging and inflammation: etiological culprits of cancer, *Curr. Aging Sci.* 2 (2009) 174–186.
- [4] H. Kühn, V.B. O'Donnell, Inflammation and immune regulation by 12/15-lipoxygenases, *Prog. Lipid Res.* 45 (2006) 334–356.
- [5] D.J. Conrad, H. Kuhn, M. Mulkins, E. Highland, E. Sigal, Specific inflammatory cytokines regulate the expression of human monocyte 15-lipoxygenase, *Proc. Natl. Acad. Sci. U. S. A.* 89 (1992) 217–221.
- [6] A.D. Dobrian, D.C. Lieb, B.K. Cole, D.A. Taylor-Fishwick, S.K. Chakrabarti, J.L. Nadler, Functional and pathological roles of the 12- and 15-lipoxygenases, *Prog. Lipid Res.* 50 (2011) 115–131.
- [7] S. Uderhardt, G. Krönke, 12/15-Lipoxygenase during the regulation of inflammation, immunity, and self-tolerance, *J. Mol. Med.* 90 (2012) 1247–1256.
- [8] A.R. Brash, Lipoxygenases: occurrence, functions, catalysis, and acquisition of substrate, *J. Biol. Chem.* 274 (1999) 23679–23683.
- [9] A. Andreou, I. Feussner, Lipoxygenases - structure and reaction mechanism, *Phytochemistry* 70 (2009) 1504–1510.
- [10] N.C. Barnes, Effects of antileukotrienes in the treatment of asthma, *Am. J. Respir. Crit. Care Med.* 161 (2000) 73–76.
- [11] J.Z. Haeggström, C.D. Funk, Lipoxygenase and leukotriene pathways: biochemistry, biology, and roles in disease, *Chem. Rev.* 111 (2011) 5866–5896.
- [12] R. Stavnichuk, V.R. Drel, H. Shevalye, I. Varenjuk, M.J. Stevens, J.L. Nadler, I.G. Obrosova, Role of 12/15-lipoxygenase in nitrosative stress and peripheral prediabetic and diabetic neuropathies, *Free Radic. Biol. Med.* 49 (2010) 1036–1045.
- [13] S.K. Chakrabarti, Y. Wen, A.D. Dobrian, B.K. Cole, Q. Ma, H. Pei, M.D. Williams, M.H. Bevard, G.E. Vandenhoff, S.R. Keller, J. Gu, J.L. Nadler, Evidence for activation of inflammatory lipoxygenase pathways in visceral adipose tissue of obese Zucker rats, *Am. J. Physiol. Endocrinol. Metab.* 300 (2011) E175–E187.
- [14] T.R. Holman, D.J. Maloney, G. Rai, A. Yagar, A. Simeonov, A. Jadhav, N. Joshi, S. Perry, G. Diaz, V. Kenyon, K. van Leyen, Q. Zhang, L. Schultz, J.E. Jung, Y. Liu, E. Lo, Potent and Selective Inhibitors Of human reticulocyte 12/15-lipoxygenase as anti-stroke therapies, *J. Med. Chem.* 57 (2014) 4035–4048.
- [15] Y.B. Joshi, P.F. Giannopoulos, D. Praticò, The 12/15-lipoxygenase as an emerging therapeutic target for Alzheimer's disease, *Trends Pharmacol. Sci.* 36 (2015) 181–186.
- [16] V.P. Chou, N. Ko, T.R. Holman, A.B. Manning-Boğ, Gene-environment interaction models to unmask susceptibility mechanisms in Parkinson's disease, *J. Vis. Exp.* 83 (2014) 1–11.
- [17] J. Ma, L. Zhang, J. Zhang, M. Liu, L. Wei, T. Shen, C. Ma, Y. Wang, Y. Chen, D. Zhu, 15-lipoxygenase-1/15-hydroxyeicosatetraenoic acid promotes hepatocellular cancer cells growth through protein kinase B and heat shock protein 90 complex activation, *Int. J. Biochem. Cell Biol.* 45 (2013) 1031–1041.
- [18] V. Salimi, M. Shabani, M. Nourbakhsh, M. Tavakoli-Yaraki, Involvement of 15-lipoxygenase-1 in the regulation of breast cancer cell death induced by sodium butyrate, *Cytotechnology* 68 (2016) 2519–2528.
- [19] I. Shureiqi, W. Jiang, X. Zuo, Y. Wu, J.B. Stimmel, L.M. Leesnitzer, J.S. Morris, H.-Z. Fan, S.M. Fischer, S.M. Lippman, The 15-lipoxygenase-1 product 13-S-hydroxyoctadecadienoic acid down-regulates PPAR-delta to induce apoptosis

- in colorectal cancer cells, *Proc. Natl. Acad. Sci. U. S. A.* 100 (2003) 9968–9973.
- [20] C. Drucker, W. Parzefall, O. Teufelhofer, M. Grusch, A. Ellinger, R. Schulte-Hermann, B. Grasl-Kraupp, Non-parenchymal liver cells support the growth advantage in the first stages of hepatocarcinogenesis, *Carcinogenesis* 27 (2006) 152–161.
- [21] L. Dubuisson, A. Monvoisin, B.S. Nielsen, B. Le Bail, P. Bioulac-Sage, J. Rosenbaum, Expression and cellular localization of the urokinase-type plasminogen activator and its receptor in human hepatocellular carcinoma, *J. Pathol.* 190 (2000) 190–195.
- [22] S. Sagmeister, M. Eisenbauer, C. Pirker, T. Mohr, K. Holzmann, H. Zwickl, C. Bichler, D. Kandjoler, F. Wrba, W. Mikulits, C. Gerner, M. Shehata, O. Majdic, B. Streubel, W. Berger, M. Micksche, K. Zatloukal, R. Schulte-Hermann, B. Grasl-Kraupp, New cellular tools reveal complex epithelial-mesenchymal interactions in hepatocarcinogenesis, *Br. J. Cancer* 99 (2008) 151–159.
- [23] H. Sadeghian, A. Jabbari, 15-Lipoxygenase inhibitors: a patent review, *Expert Opin. Ther. Pat.* 26 (2016) 65–88.
- [24] A. Bräthe, G. Andresen, L.L. Gundersen, K.E. Malterud, F. Rise, Antioxidant activity of synthetic cytokinin analogues: 6-Alkynyl- and 6-alkenylpurines as novel 15-lipoxygenase inhibitors, *Bioorg. Med. Chem.* 10 (2002) 1581–1586.
- [25] V. Kenyon, I. Chorny, W.J. Carvajal, T.R. Holman, M.P. Jacobson, Novel human lipoxygenase inhibitors discovered using virtual screening with homology models, *J. Med. Chem.* 49 (2006) 1356–1363.
- [26] D.S. Weinstein, W. Liu, Z. Gu, C. Langevine, K. Ngu, L. Fadnis, D.W. Combs, D. Sitkoff, S. Ahmad, S. Zhuang, X. Chen, F.L. Wang, D.A. Loughney, K.S. Atwal, R. Zahler, J.E. Macor, C.S. Madsen, N. Murugesan, Tryptamine and homotryptamine-based sulfonamides as potent and selective inhibitors of 15-lipoxygenase, *Bioorg. Med. Chem. Lett.* 15 (2005) 1435–1440.
- [27] N. Eleftheriadis, C.G. Neochoritis, N.G.J. Leus, P.E. Van Der Wouden, A. Dömling, F.J. Dekker, Rational development of a potent 15-lipoxygenase-1 inhibitor with in vitro and ex vivo anti-inflammatory properties, *J. Med. Chem.* 58 (2015) 7850–7862.
- [28] N. Eleftheriadis, H. Poelman, N.G.J. Leus, B. Honrath, C.G. Neochoritis, A. Dolga, A. Dömling, F.J. Dekker, Design of a novel thiophene inhibitor of 15-lipoxygenase-1 with both anti-inflammatory and neuroprotective properties, *Eur. J. Med. Chem.* 122 (2016) 786–801.
- [29] C. Abad-Zapatero, J.T. Metz, Ligand efficiency indices as guideposts for drug discovery, *Drug Discov. Today* 10 (2005) 464–469.
- [30] J. Baell, M.A. Walters, Chemical con artists foil drug discovery, *Nature* 513 (2014) 481–483.
- [31] J.B. Baell, G.A. Holloway, New substructure filters for removal of pan assay interference compounds (PAINS) from screening libraries and for their exclusion in bioassays, *J. Med. Chem.* 53 (2010) 2719–2740.
- [32] N. Eleftheriadis, S.A. Thee, M.R.H. Zwiderman, N.G.J. Leus, F.J. Dekker, Activity-based probes for 15-lipoxygenase-1, *Angew. Chem. Int. Ed.* 55 (2016) 12300–12305.
- [33] V. Nagarajan, R.W. Fessenden, Flash photolysis of transient radicals. Benzophenone Ketyl radical, *Chem. Phys. Lett.* 112 (1984) 207–211.
- [34] B.W. Hodgson, J.P. Keene, E.J. Land, A.J. Swallow, Light-induced fluorescence of short-lived species produced by a pulse of radiation: the benzophenone ketyl radical, *Am. Inst. Phys.* 3671 (1975).
- [35] L.V. Frolova, N.M. Evdokimov, K. Hayden, I. Malik, S. Rogelj, A. Kornienko, I.V. Magedov, One-pot multicomponent synthesis of diversely substituted 2-aminopyrroles. A short general synthesis of rigidins A, B, C, and D, *Org. Lett.* 13 (2011) 1118–1121.
- [36] K. Wang, A. Dömling, Design of a versatile multicomponent reaction leading to 2-amino-5-ketoaryl pyrroles, *Chem. Biol. Drug Des.* 75 (2010) 277–283.
- [37] M.T. Cocco, C. Congiu, V. Onnis, Synthesis and in vitro antitumoral activity of new N -Phenyl-3-pyrrolocarbothioamides, *Bioorg. Med. Chem.* 11 (2003) 495–503.
- [38] V. Onnis, A. De Logu, M.T. Cocco, R. Fadda, R. Meleddu, European journal of medicinal chemistry 2-Acylhydrazino-5-arylpyrrole derivatives: synthesis and antifungal activity evaluation, *Eur. J. Med. Chem.* 44 (2009) 1288–1295.
- [39] C.H. Lieu, P.J. Klauck, P.K. Henthorn, J.J. Tentler, C. Tan, A. Spreafico, H.M. Selby, B.C. Britt, S.M. Bagby, J.J. Arcaroli, W.A. Messersmith, T.M. Pitts, S.G. Eckhardt, Antitumor activity of a potent MEK inhibitor, TAK-733, against colorectal cancer cell lines and patient derived xenografts, *Oncotarget* 6 (2015) 34561–34572.
- [40] M. Tanaka, Y. Sasaki, Y. Kimura, T. Fukui, K. Hamada, Y. Ukai, A novel pyrrole derivative, NS-8, suppresses the rat micturition reflex by inhibiting afferent pelvic, *BJU Int.* 92 (2003) 1031–1036.
- [41] T. Dougherty, S. Schwartz, Photodynamic Therapy for Cancer Skin of Mice, vol. 3, 2003, pp. 380–387.
- [42] K. Traven, N. Eleftheriadis, S. Serßen, J. Kljun, J. Bezenšek, B. Stanovnik, I. Turel, F.J. Dekker, Ruthenium complexes as inhibitors of 15-lipoxygenase-1, *Polyhedron* 101 (2015) 306–313.